

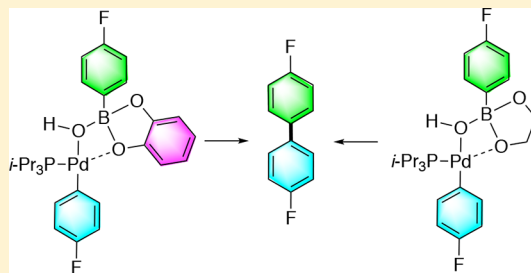
Elucidating the Role of the Boronic Esters in the Suzuki–Miyaura Reaction: Structural, Kinetic, and Computational Investigations

Andy A. Thomas,^{ID} Andrew F. Zahrt, Connor P. Delaney, and Scott E. Denmark^{*ID}

Roger Adams Laboratory, Department of Chemistry, University of Illinois, Urbana, Illinois 61801, United States

Supporting Information

ABSTRACT: The Suzuki–Miyaura reaction is the most practiced palladium-catalyzed, cross-coupling reaction because of its broad applicability, low toxicity of the metal (B), and the wide variety of commercially available boron substrates. A wide variety of boronic acids and esters, each with different properties, have been developed for this process. Despite the popularity of the Suzuki–Miyaura reaction, the precise manner in which the organic fragment is transferred from boron to palladium has remained elusive for these reagents. Herein, we report the observation and characterization of pretransmetalation intermediates generated from a variety of commonly employed boronic esters. The ability to confirm the intermediacy of pretransmetalation intermediates provided the opportunity to clarify mechanistic aspects of the transfer of the organic moiety from boron to palladium in the key transmetalation step. A series of structural, kinetic, and computational investigations revealed that boronic esters can transmetalate directly without prior hydrolysis. Furthermore, depending on the boronic ester employed, significant rate enhancements for the transfer of the B-aryl groups were observed. Overall, two critical features were identified that enable the transfer of the organic fragment from boron to palladium: (1) the ability to create an empty coordination site on the palladium atom and (2) the nucleophilic character of the *ipso* carbon bound to boron. Both of these features ultimately relate to the electron density of the oxygen atoms in the boronic ester.



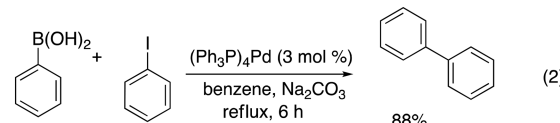
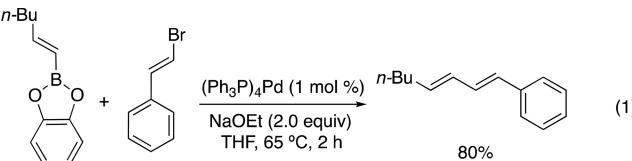
1. INTRODUCTION

The Suzuki–Miyaura reaction is the most practiced carbon–carbon bond forming reaction in both academic and industrial settings.¹ The impact of this tremendously enabling process was recognized by inclusion in the 2010 Nobel Prize in Chemistry. The success of this unique coupling technology derives from the innate ability of the organoboron donor reagents to undergo transmetalation with transition metals such as palladium. Moreover, these reagents are straightforward to prepare, exceptionally stable, environmentally benign and commercially available.² In 1979, the first reported coupling combined catechol alkenylboronic esters and bromoalkenes in the presence of a palladium catalyst and base (Scheme 1, 1).³ Later in 1981, Suzuki and Miyaura demonstrated that boronic acids could also undergo cross-coupling reactions with organohalides (Scheme 1, 2).⁴

Currently, boronic acids are the most commonly employed coupling partners because of their ease of preparation and high atom economy as is illustrated in various commercial syntheses such as for the BASF fungicide boscalid⁵ (Figure 1).

Boronic esters, especially pinacol boronic esters, have been employed as late stage coupling partners in many syntheses of active pharmaceutical agents.⁶ Two illustrative examples from Abbott Laboratories include the synthesis of kinase inhibitor ABT-869, which is being developed as a chemotherapeutic agent and diacyl glycerol acyltransferase inhibitor DGAT-1.^{7,8} Additionally, a potent and selective mesenchymal epithelial transition factor/anaplastic lymphoma kinase inhibitor (Crizotinib) has

Scheme 1. Original Suzuki–Miyaura Coupling Conditions



been synthesized by a late stage Suzuki–Miyaura coupling employing a pinacol boronic ester (Figure 1).⁹

However, boronic acids and esters are not without limitations. For example, coupling partners such as vinyl, cyclopropyl, electron-rich heterocyclic derivatives and electron-deficient arylboronic acids are prone to undergo protodeboronation.¹⁰ As these building blocks are ubiquitous in active pharmaceutical agents, intense effort over the past 40 years has gone into the development of a variety of masked reagents¹¹ (e.g., boronic esters, trifluoroboronates, MIDA boronates, etc.) that provide both increased shelf life and stability under basic reaction conditions (Figure 2). These masked reagents are presumed to

Received: January 16, 2018

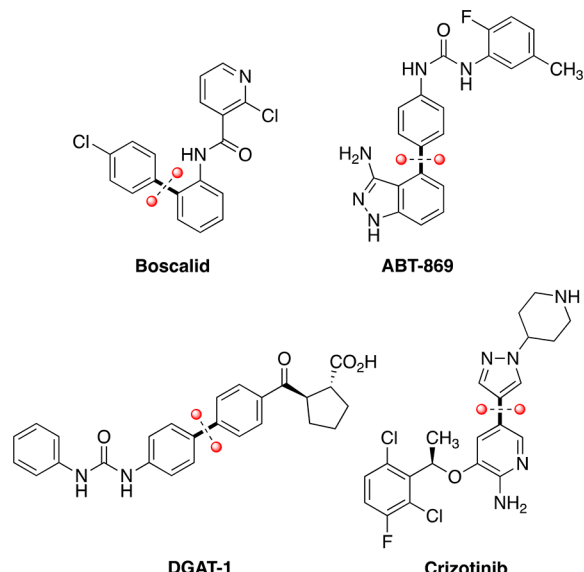


Figure 1. Examples of late stage coupling with boronic acids and esters.

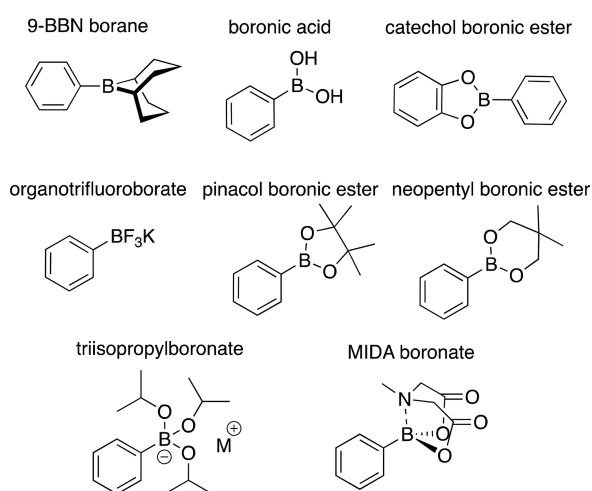


Figure 2. Examples of some of the most popular boron coupling partners.

work by slowly revealing the corresponding boronic acid by hydrolysis under typical aqueous basic reaction conditions. Recent investigations by Lloyd-Jones et al. have shown that in certain cases such as trifluoroboronate salts¹² as well as MIDA boronates¹³ a hydrolysis step is required prior to the transmetalation event.

Although the organoboron reagents mentioned above have all been documented to operate successfully under Suzuki–Miyaura reaction conditions, the precise manner in which certain reagents undergo the crucial transmetalation event remains obscure. A recent review by Lennox and Lloyd-Jones states that “Evidently boronic esters exhibit greater stability than their corresponding boronic acids, but it is not clear what the active transmetalating species is during their Suzuki–Miyaura coupling.”¹⁴

2. BACKGROUND

Previous reports from these laboratories described the first structure elucidation and kinetic behavior of pretransmetalation intermediates, “The Missing Links”, in the Suzuki–Miyaura reaction between arylboronic acids and arylpalladium complexes.¹⁵ Specifically, the combination of dimeric complex $[(i\text{-Pr}_3\text{P})(4\text{-FC}_6\text{H}_4)\text{Pd}(\text{OH})]_2$ (**1**) with 4-fluorophenylboronic acid (**2**) (1.0 equiv/Pd) in THF at low temperature resulted in the observation and characterization of complex **3** with a 2:1 stoichiometry (Pd/B), Figure 3a. However, prior to the crucial transmetalation event, complex **3** was kinetically and computationally shown to convert to 8-B-4¹⁶ complex **4**. Additionally, palladium complexes bearing various phosphine ligands such as Ph_3P , $i\text{-Pr}_3\text{P}$, and DPPF were found to form species containing Pd–O–B linkages that could be kinetically monitored to form cross-coupling product **5**, Figure 3b. The rate of the transmetalation process followed the trend $\text{Ph}_3\text{P} > i\text{-Pr}_3\text{P} > \text{DPPF}$, highlighting the need for generating a coordinatively unsaturated and electrophilic palladium atom during the transmetalation process.

The formation of 2:1 complex **3** raised a number of questions regarding the origin of its stability. Because this structure is heavily dependent upon the bridging capability of various oxygen atoms, it seemed logical to examine the effect of other donors. Interestingly, the addition of CD_3OD into a $\text{THF}-d_8$ solution containing complex **3** (from **1** and **2**, *vide supra*) with 1.0 equiv of **2** at -55°C resulted in the quantitative formation of 1:1 complex **6**, Scheme 2, left. An independent synthesis confirmed the identity of complex **6** by combining dimethyl 4-fluorophenyl boronic ester (**7**) (1.0 equiv/Pd) with palladium dimer **1** in $\text{THF}-d_8/\text{CD}_3\text{OD}$. After being warmed to -55°C , the quantitative formation of complex **6** was observed indicating that methanol was incorporated into the structure (Scheme 2, right).

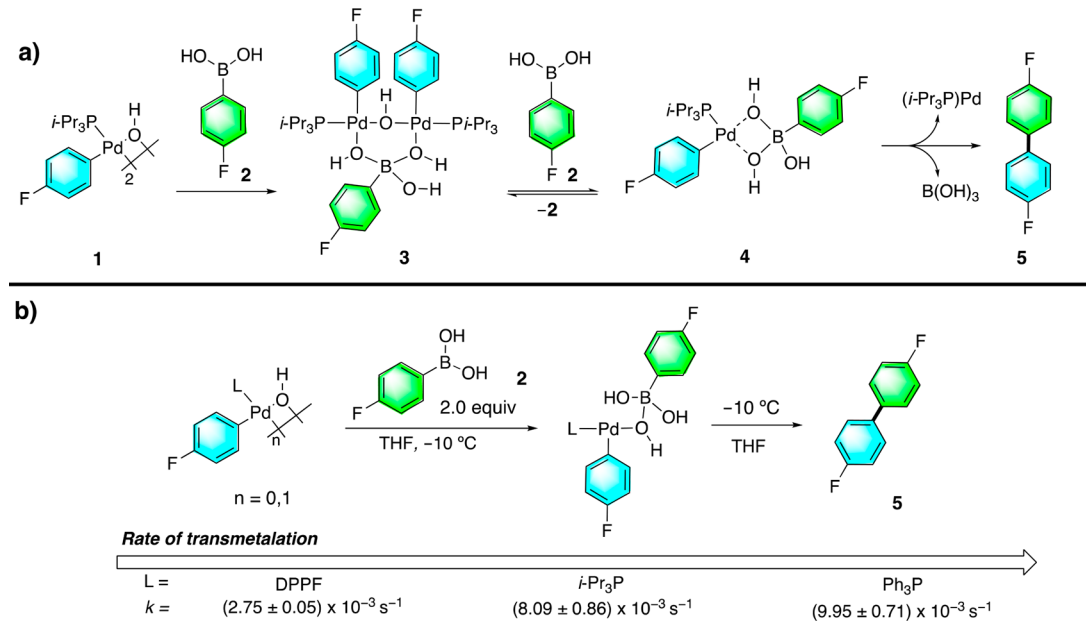
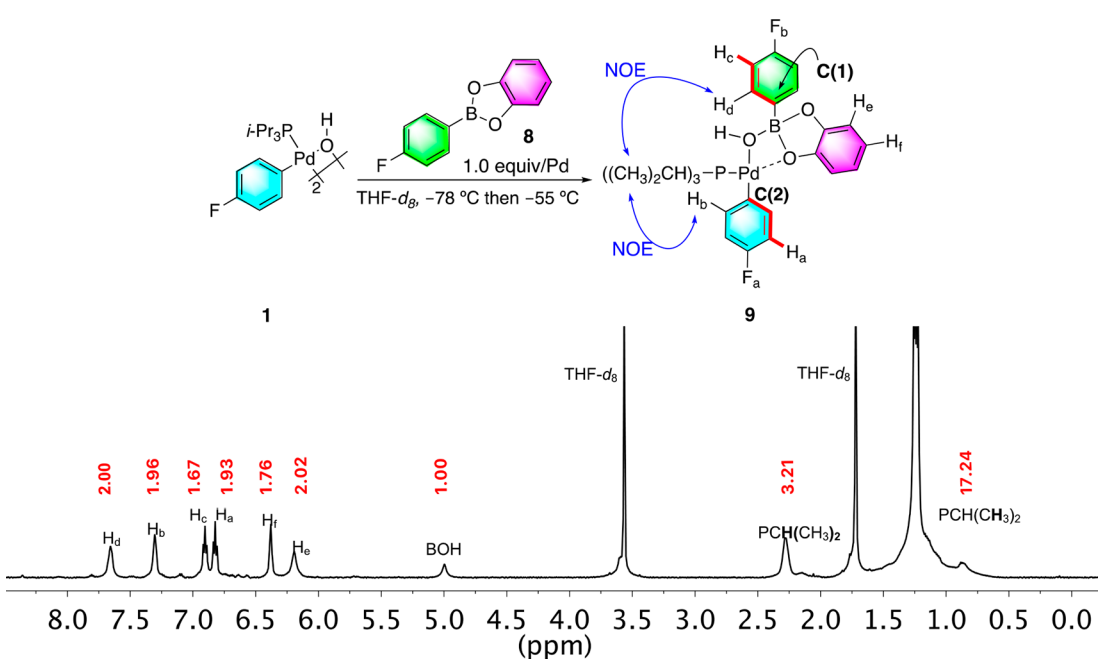
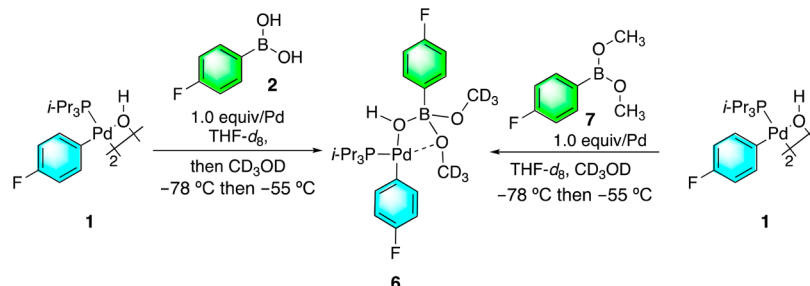
3. GOALS OF THIS STUDY

Following the successful formation of pretransmetalation intermediates with arylboronic acids, we sought to investigate whether pretransmetalation intermediates could be formed which incorporate some of the most common arylboronic esters (catechol, isopropyl, and pinacol etc.) employed in the Suzuki–Miyaura reaction. The specific goals include: (1) full characterization of the pretransmetalation species, (2) demonstration of the kinetic competence of the characterized species containing Pd–O–B linkages to form cross-coupling product, and (3) quantum mechanical simulation of the transmetalation process involving these intermediates.

4. RESULTS AND DISCUSSION

4.1. Preparation and Structural Analysis of Pd–O–B Complexes. **4.1.1. Reaction of $[(i\text{-Pr}_3\text{P})(4\text{-FC}_6\text{H}_4)\text{Pd}(\text{OH})]_2$ with Various Catechol 4-Fluorophenylboronic Esters.** Previous investigations that employed $[(i\text{-Pr}_3\text{P})(4\text{-FC}_6\text{H}_4)\text{Pd}(\text{OH})]_2$ (**1**) and dimethyl 4-fluorophenylboronic ester (**7**) in $\text{THF}/\text{CH}_3\text{OH}$ as described above directed us to investigate the interaction between catechol 4-fluorophenylboronic ester (**8**) and palladium complex **1** using variable temperature NMR spectroscopy.^{15b} The catechol boronic ester embodies decidedly different steric and electronic properties compared to a dimethyl ester and thus would signal any consequences arising from the presence of the ester group in the transmetalation event.

Addition of a $\text{THF}-d_8$ solution of catechol boronic ester **8** (1.0 equiv/Pd) to a $\text{THF}-d_8$ solution of dinuclear complex **1** at -78°C followed by warming to -55°C produced a single, new complex **9** by ^1H NMR spectroscopy (Figure 4).¹⁷ The identity of a union between the starting materials, a “Pd–O–B linkage”, was established by the observation of strong through space interactions between the aryl protons (H_b and H_d) and the

**Figure 3.** Pretransmetalation intermediates formed with arylboronic acids.**Scheme 2. Formation of 8-B-4 Complex 5****Figure 4.** Formation of a catechol boronate pretransmetalation intermediate 9 and its ¹H NMR spectrum. Integrals are reported in red.

methyl hydrogens on the *i*-Pr₃P group. However, NOE cross-peaks were absent between the *i*-Pr₃P methyl groups and the

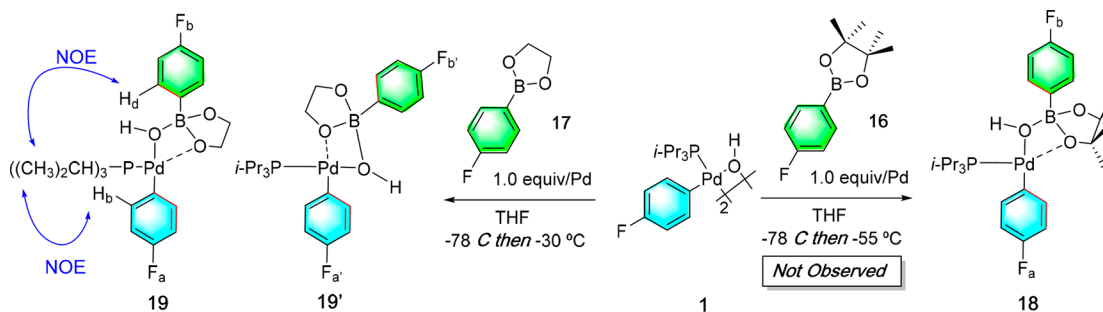
catechol hydrogens (H_e and H_f) suggesting a *trans* relationship between the *i*-Pr₃P ligand and catechol backbone. This

Table 1. ^{19}F NMR Chemical Shifts (ppm) for Catechol Ester Pretransmetalation Intermediates

1

entry	complex	R	R ₁	R ₂	R ₃	F_a	F_b
1	9	H	H	H	H	-120.77	-117.43
2	11	Cl	Cl	Cl	Cl	-120.93	-118.27
3	14	H	MeO	MeO	H	-120.96	-117.51
4	15	MeO	H	H	MeO	-121.59	-117.64

Scheme 3. Formation of 8-B-4 Complexes with Glycol and Pinacol Boronic Esters



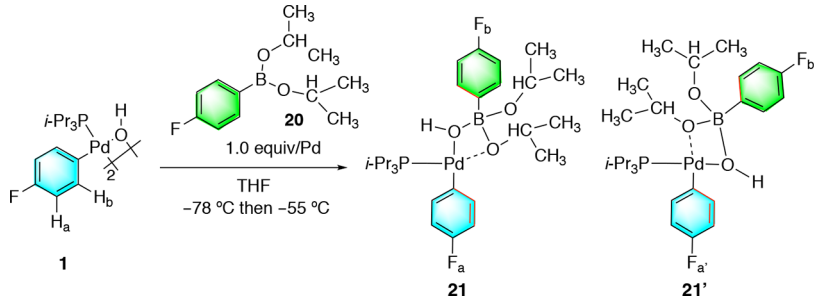
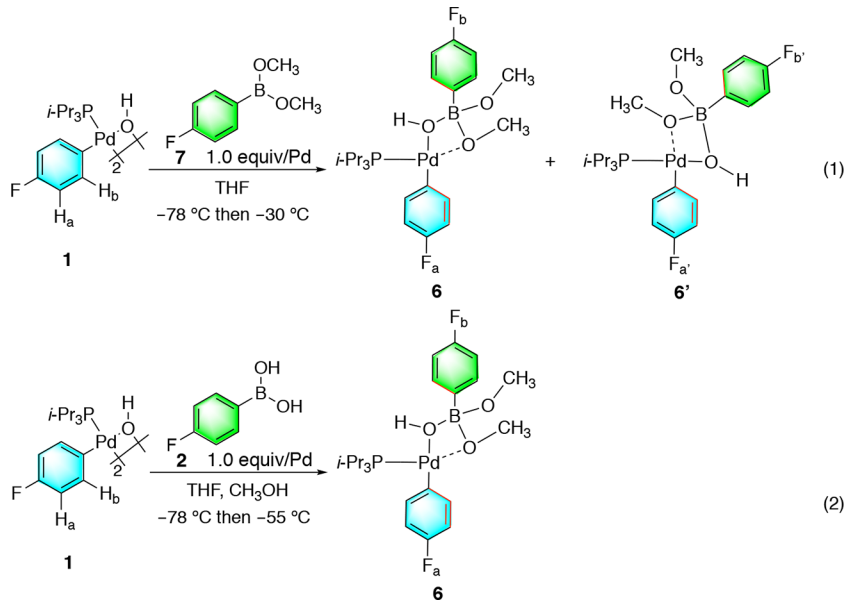
hypothesis found further support in the computationally derived ground states where a 1.9 kcal/mol energy difference favoring the *trans* configuration was found, (cf. Section 4.4). The *ipso* carbon atoms bonded to the boron and palladium atoms C(1) and C(2), which do not appear in the ^{13}C NMR spectrum, were revealed in the HMBC (^1H – ^{13}C) spectrum by the observation of cross peaks between H_c and H_a hydrogens with the ^{13}C signals at 144.52 ppm (C(1)) and 136.85 ppm (C(2)), respectively (red bonds). Finally, the coordination environment about the boron atom was confirmed in the ^{11}B NMR spectrum in which a broad signal was observed at 12 ppm, a 20 ppm $\Delta(^{11}\text{B})$ upfield shift compared to unbound 8, indicating that the geometry about the boron atom had changed from tricoordinate to tetracoordinate.¹⁸

The facile formation of 9 containing a Pd–O–B linkage led us to investigate whether similar species could be observed using modified catechol boronic esters. Interestingly, the addition of electron deficient tetrachlorocatechol 4-fluorophenylboronic ester **10** (1.0 equiv/Pd) to complex **1** at -78°C followed by warming to -30°C resulted in the formation of a single new species **11** by ^{19}F NMR spectroscopy (-120.93 ppm (F_a), -118.27 ppm (F_b) (Table 1). Additionally, both 4,5-dimethyoxycatechol and 3,6-dimethyoxycatechol 4-fluorophenylboronic esters **12** and **13** also quantitatively formed new complexes at -30°C by ^{19}F NMR spectroscopy. These results indicate that the electronic properties of the catechol residue do not deter the formation of related intermediates. We next investigated the behavior of aliphatic, 5-membered ring containing pinacol (**16**) and glycol (**17**) 4-fluorophenylboronic esters, respectively.

4.1.2. Reaction of $[(i\text{-Pr}_3\text{P})(4\text{-FC}_6\text{H}_4)\text{Pd}(\text{OH})]_2$ with Pinacol and Glycol 4-Fluorophenylboronic Esters. The addition of pinacol boronic ester **16** (1.0 equiv/Pd) to complex **1** at -78°C

followed by warming to -55°C in THF resulted in no observable complex formation by ^{19}F NMR spectroscopy (Scheme 3, right). Even upon warming to -30°C , no intermediate was observed; however, slow formation of cross-coupling product **5** was seen (cf. Section 4.2.2).¹⁹ The lack of a discrete intermediate was attributed to the steric bulk around the boron atom imparted by the methyl substituents on the pinacol boronic ester. Consequently, investigation of the less sterically encumbered glycol boronic ester (**17**) was undertaken.

Addition of a THF solution of glycol boronic ester **17** (1.0 equiv/Pd) to complex **1** in THF at -78°C followed by warming to -55°C resulted in the conversion of the starting materials to two new complexes by ^{19}F NMR spectroscopy in a $\sim 90:10$ ratio (Scheme 3, left). However, the complexes were too reactive at this temperature for complete characterization. The mixture was therefore first generated at -78°C , briefly annealed at -70°C , and was subsequently cooled to -80°C . At this temperature, the complexes were stable for ca. 4 h, allowing ^1H NMR and NOE spectra to be acquired thus enabling more secure structural assignments. The connectivity of the complexes through a Pd–O–B linkage was confirmed by the observation of strong through space interactions between the aryl protons (H_b and H_d) and the methyl hydrogens on the *i*-Pr₃P group. The major species **19** (^{19}F NMR signals at -122.00 ppm (F_a) and -118.74 (F_b)) was assigned as the expected T-shaped complex with the glycol oxygen bound *trans* to the *i*-Pr₃P ligand. The minor species **19'** (^{19}F NMR signals at -122.24 ppm ($F_{a'}$) and -119.36 ppm ($F_{b'}$)) was tentatively assigned as the isomeric complex in which the glycol substituent is *cis* to the *i*-Pr₃P ligand (Scheme 3, left).²⁰ Although a ^{11}B NMR spectrum could not be obtained at -80°C , the ^1H spectrum revealed four distinct resonances for the 1,3,2-

Scheme 4. Formation of an 8-B-4 Complex with a Diisopropyl Boronic Ester**Scheme 5.** Formation of 8-B-4 Complexes with a Dimethyl Boronic Ester

dioxaborolane ring, implying that the boron is in a 4-coordinate state to break the symmetry of the ring. Together, this evidence strongly suggests the formation of a Pd–O–B linked species containing glycol boronic ester 17. The observation of this intermediate confirms that the pinacol boronic ester 16 was indeed too hindered to allow complexation.

4.1.3. Reaction of $[(i\text{-Pr}_3\text{P})(4\text{-FC}_6\text{H}_4)\text{Pd}(\text{OH})_2]$ with Diisopropyl and Dimethyl 4-Fluorophenylboronic Esters. Following the established protocol, 1.0 equiv/Pd of diisopropyl boronic ester 20 was combined with palladium complex 1 in THF at -78°C followed by warming to -55°C . ^{19}F NMR spectroscopic analysis showed a $\sim 50\%$ conversion of the starting materials to two new species in a ca. 50:50 ratio (**Scheme 4**). The first set of signals was assigned to complex 21 at -123.58 ppm (F_{a}) and -115.08 ppm (F_{b}). The second set of signals was assigned as complex 21' at -123.18 ppm ($F_{\text{a}'}$) and -114.42 ppm ($F_{\text{b}'}$). Interestingly, allowing the reaction mixture to sit at -55°C for $\sim 1\text{ h}$ did not result in any further incorporation of diisopropyl boronic ester 20 into the dimeric palladium complex indicating that the system was at equilibrium. Warming the sample to -30°C resulted in the formation of cross-coupling product 5 (**Section 4.2.3**). The observation of two intermediates with diisopropyl boronic ester 20 supported our conclusion that pinacol boronic ester 16 was too sterically congested to form an adduct. Accordingly, the acyclic analog of the glycol boronic ester 17, namely the dimethyl 4-fluorophenylboronate (7) was examined next.

The addition of a THF solution of dimethyl boronic ester 7 (1.0 equiv/Pd) to a THF solution of palladium complex 1 at -78°C followed by warming to -30°C resulted in an $\sim 60\%$ conversion of 1 to two new complexes in a ratio of 65:35 as evidenced by the observation of two new sets of ^{19}F NMR signals. The first set of signals at -121.58 ppm (F_{a}) and -118.85 ppm (F_{b}) was assigned to complex 6. The second set of signals at -121.13 ppm ($F_{\text{a}'}$) and -118.72 ppm ($F_{\text{b}'}$) was assigned as complex 6' (**Scheme 5-1**).²¹ The observation of two complexes was surprising because only one dimethyl boronic ester complex was observed in THF/CH₃OH (9:1) suggesting that excess methanol provides a pathway for the minor complex 6' to convert to complex 6 (**Scheme 5-2**).

4.2. Kinetic Analysis of the Pretransmetalation Complexes. To establish the effect of the boronic ester moiety on the rate of transmetalation, 8-B-4 complexes were freshly generated in THF at -78°C followed by warming to -30°C such that the evolution of their ^{19}F NMR signals could be monitored. The formation of cross-coupling product 5 from each complex followed clean, first-order behavior thus providing accurate values for k (**Table 2**).²² Previously, arylboronic acid 2 was found to form cross-coupling product 5 at a rate of $(5.78 \pm 0.13 \times 10^{-4}\text{ s}^{-1})$ (**Table 2**, entry 1).¹⁵ To allow for a straightforward comparison of the arylboronic ester substrates described below, the rates were normalized to the arylboronic acid 2 (**Table 2**, entry 1). In addition to the arylboronic esters described in the previous section, a number of other esters possessing diverse

Table 2. Effect of the Arylboronic Ester on the Rate of Transmetalation

entry	substrate	complex	^a form k, 10 ⁻³ s ⁻¹	k _{rel}
1			0.578 ± 0.013	1.00
2			2.46 ± 0.39	4.27
3			0.0013 ± 0.0004	0.0022
4			2.73 ± 0.54	4.20
5			3.34 ± 0.21	5.78
6 ^b			—	—
7 ^b			—	—
8			0.824 ± 0.016	1.42
9			13.3 ± 0.7	23.01
10			12.4 ± 0.2	21.45
11 ^b			5.39 ± 0.07	9.33
12			0.226 ± 0.031	0.39

^aAverage of triplicate runs. ^bNo intermediate was detected.

steric and electronic properties were also investigated to probe the influence of the ester on the rate of the transmetalation event. The preparation of these esters is described in the Supporting Information.

4.2.1. Effect of Catechol Arylboronic Esters on the Rate of Transmetalation. Interestingly, catechol complex **9** was found to undergo transmetalation ~4.3 times faster than the

arylboronic acid complex **4**, indicating that the catechol moiety is a contributing component in the transmetalation event (Table 2, entry 2).²³ To probe the effects of the catechol residue, a series of electronically modulated catechol esters was investigated.

Upon generation of electron deficient tetrachlorocatechol 4-fluorophenylboronate complex **11** from **1** and **10** at -30 °C, no cross-coupling product **5** was formed. Therefore, to obtain a rate

Scheme 6. Reaction of Palladium Complex 1 with Boronic Esters 15 and 24

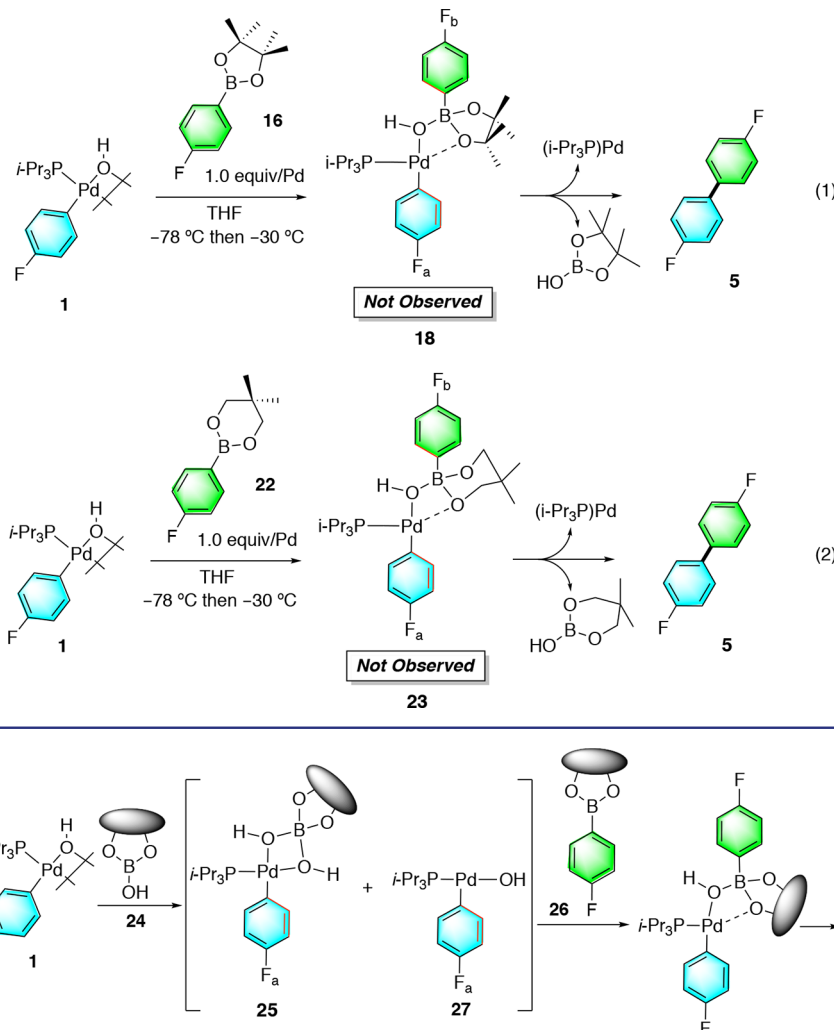


Figure 5. Proposed mechanism of cross-coupling formation with pinacol ester 15 and dimeric palladium complex 1.

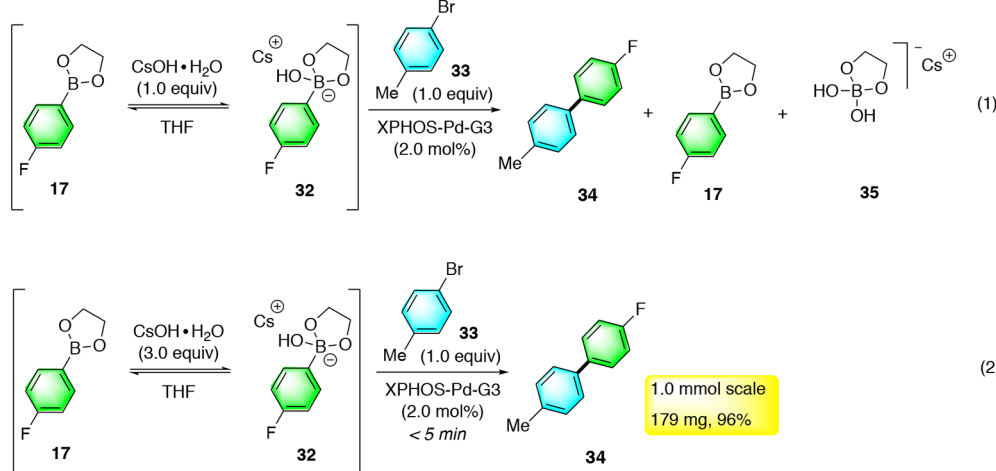
constant that could be compared at $-30\text{ }^{\circ}\text{C}$, an Eyring analysis was performed over a range of higher temperatures (-5 to $20\text{ }^{\circ}\text{C}$) which allowed for a k value to be extracted ($1.30 \pm 0.40 \times 10^{-6}\text{ s}^{-1}$) (Table 2, entry 3). The sluggish reactivity of 11 clearly demonstrated that the electron deficiency of catechol ester moiety severely attenuated the migratory ability of the aryl ring compared to complex 9. Combining dimeric palladium complex 1 with 4,5-dimethyoxycatechol- and 3,6-dimethyoxycatechol 4-fluorophenylboronic esters 12 and 13, similar transmetalation rates were observed: ($2.43 \pm 0.54 \times 10^{-3}\text{ s}^{-1}$) 14 and ($3.34 \pm 0.31 \times 10^{-3}\text{ s}^{-1}$) 15, respectively (Table 2, entries 4 and 5). Although both complexes reacted more rapidly than arylboronic acid complex 4, the effective rate increase was only 4.20 and 5.78 respectively, suggesting that electron-donating substituents are less influential than electron-withdrawing substituents. The next line of investigation addressed boronate complexes derived from boronic acid esters bearing aliphatic diols and alcohols.

4.2.2. Effect of Pinacol and Neopentyl Arylboronic Esters on the Rate of Transmetalation. Attempts to measure rates for the formation of cross-coupling product 5 from pinacol and neopentyl boronic esters 16 and 22 with dimeric palladium complex 1 resulted in sigmoidal kinetic profiles that could not be fit using a first-order decay (Scheme 6).²⁴ However, the pinacol and neopentyl boronic esters did react, albeit at very different

rates, ~ 5.5 and $\sim 0.3\text{ h}$ respectively, to form product 5 whereas the arylboronic acid 2 took roughly $\sim 1.2\text{ h}$.

The observation of sigmoidal kinetic profiles suggests that one of the reaction products was influencing the rate of transmetalation. One possible explanation is that following transmetalation the boronic acid byproduct 24 breaks the Pd–(μ OH)–Pd bond in dimeric palladium complex 1 to form a new complex 25, which provides a pathway for the arylboronic ester 26 to bind T-shaped complex 27 (Figure 5).²⁵ These results suggest that complexation is crucial for the transmetalation event to take place. As described in Section 4.1.3, an acyclic analog of pinacol boronic ester 16, namely diisopropyl boronic ester 20, was able to form a discrete intermediate at low temperature; therefore, it was examined next.

4.2.3. Effect of the Diisopropyl Arylboronic Ester on the Rate of Transmetalation. Preparing diisopropyl complex 21 from 1 and 20 at $-30\text{ }^{\circ}\text{C}$ resulted in the observation of cross-coupling product 5 at $k = 8.24 \pm 0.16 \times 10^{-4}\text{ s}^{-1}$, which was only slightly faster (1.42) than the arylboronic acid complex 4 (Table 2, entry 8). Because the observed rate is directly proportional to the concentration of complex 21 (rate = $k_{\text{obs}}[\text{A}]$), the incomplete formation of 21 in the pre-equilibrium (see Section 4.1.3) likely causes the diminished rate.²⁶ Thus, our investigations shifted to

Scheme 7. Cross-Coupling of Glycol Ester 16 in a Catalytic Reaction

glycol and dimethyl boronic esters **17** and **7** which form intermediates quantitatively.

4.2.4. Effect of the Glycol and Dimethyl Arylboronic Esters on the Rate of Transmetalation. Warming a solution of glycol boronic ester complex **19** to $-30\text{ }^{\circ}\text{C}$ provided a first-order rate constant of $k = 13.3 \pm 0.70 \times 10^{-3} \text{ s}^{-1}$ for the formation of cross-coupling product **5** (**Table 2**, entry 9). Remarkably, the glycol boronic ester complex **19** transferred its aryl group ~ 23 times faster than the arylboronic acid complex **4** (~ 5.0 times faster than the catechol boronic ester complex **9**, indicating that the glycol moiety greatly influenced the rate of transmetalation. To probe the origin of the rate enhancement, the dimethyl boronic ester **7** was investigated to evaluate the contribution from the conformationally restricted glycol moiety.

Formation of cross-coupling product **5** from dimethyl boronic ester complex **6** resulted in the observation of 21-fold rate increase compared to the arylboronic acid complex **4** (**Table 2**, entry 10), suggesting that the conformational restriction imposed by the glycol boronic ester was not a significant contributor to the observed rate enhancement.

The observed acceleration of the transmetalation step with simple aliphatic esters (compared to the parent boronic acid) is clearly arising from a combination of factors because both electron deficient (catechol) and electron rich (glycol) esters led to increased rates. Therefore, to gain further insight into the influence of the Lewis basicity of the boronate oxygen atoms on the transmetalation rate, electron deficient boroxine **28** and α -hydroxy isobutyrate 4-fluorophenylboronic ester **29** were examined next.

4.2.5. Effect of Boroxine and α -Hydroxyisobutyrate Boronic Ester on the Rate of Transmetalation. Following the standard protocol, the addition of boroxine **28** to dimeric complex **1** resulted in the formation of cross-coupling product **5** at a rate of $5.39 \pm 0.07 \times 10^{-3} \text{ s}^{-1}$. Intriguingly, though a discrete intermediate was not observed²⁷ the rate was ~ 9.33 times faster than the arylboronic acid complex **4** (**Table 2**, entry 11).

Next, upon combination of α -hydroxyisobutyrate boronic ester **29** with complex **1** at $-78\text{ }^{\circ}\text{C}$ a new complex, **31** was observed. Warming **31** to $-30\text{ }^{\circ}\text{C}$ resulted in the formation of cross-coupling product **5** with first-order rate constant of $2.26 \pm 0.31 \times 10^{-4} \text{ s}^{-1}$. Whereas this complex reacted more slowly ($k_{\text{rel}} = 0.39$) than arylboronic acid **2**, it was considerably faster than the pinacol ester **16**.

4.2.6. Comparison of Arylboronic Esters on Rate of Transmetalation. The goal of the kinetic experiments outlined above was to identify those structural and electronic effects that influence the transmetalation rate. Specifically, three important observations were made: (1) certain hindered esters (pinacol and diisopropyl) do not quantitatively form 8-B-4 complexes containing Pd–O–B linkages and therefore are less reactive than the others,²⁷ (2) electron deficient esters (catechol and boroxine) led to a rate increase when compared to the boronic acid, and (3) electron rich esters (glycol, neopentyl, and dimethyl) led to increased rates when compared to the boronic acid. Taken together, it is clear that multiple features of the boronic ester are responsible for the rate of aryl migration. Three primary factors can be identified: (1) the ease of rehybridization of the boron atom which in turn is affected by the steric accessibility, electrophilicity, and angular distortion of the boron atom, (2) the ease of formation of a coordinatively unsaturated palladium complex which in turn is affected by the Lewis basicity and steric demand of the oxygen atoms, and (3) migratory aptitude of the aryl group which in turn is also affected by the Lewis basicity of the oxygen atoms, but with inverse dependence compared to factor 2. Thus, to identify the relative contribution of all of these factors, a thorough computational analysis was performed on the reaction coordinates for complexes **4**, **9**, and **19** (**Section 4.4**).

4.3. Demonstration of a Catalytic Reaction. It is of paramount importance to establish whether this rate increase would be manifested under preparative, catalytic conditions. Our observations support the previous findings that the main role of base in the Suzuki–Miyaura reaction is to convert the oxidative addition product ArPdX to the competent ArPdOH species when aqueous mixtures are employed (path B).²⁸ However, previous investigations from these laboratories demonstrated that under certain conditions the oxidative addition product ArPdX could react directly with ArYL(OH)₃X to form Pd–O–B linkages (path A).¹⁵ Because catalytic reactions must be run under anhydrous conditions (to avoid hydrolysis of the ester) with a stoichiometric amount of base, we suspected that the combination of glycol boronic ester **17** with CsOH·H₂O might allow for a soluble 8-B-4 hydroxy glycol boronate **32** to be formed which would allow access to path A.²⁹ Indeed, mixing 1.0 equiv of CsOH·H₂O with glycol boronic ester **17** in THF resulted in the formation of 8-B-4 hydroxy glycol boronate **32** (**Scheme 7-1**). Upon addition of a THF solution employing

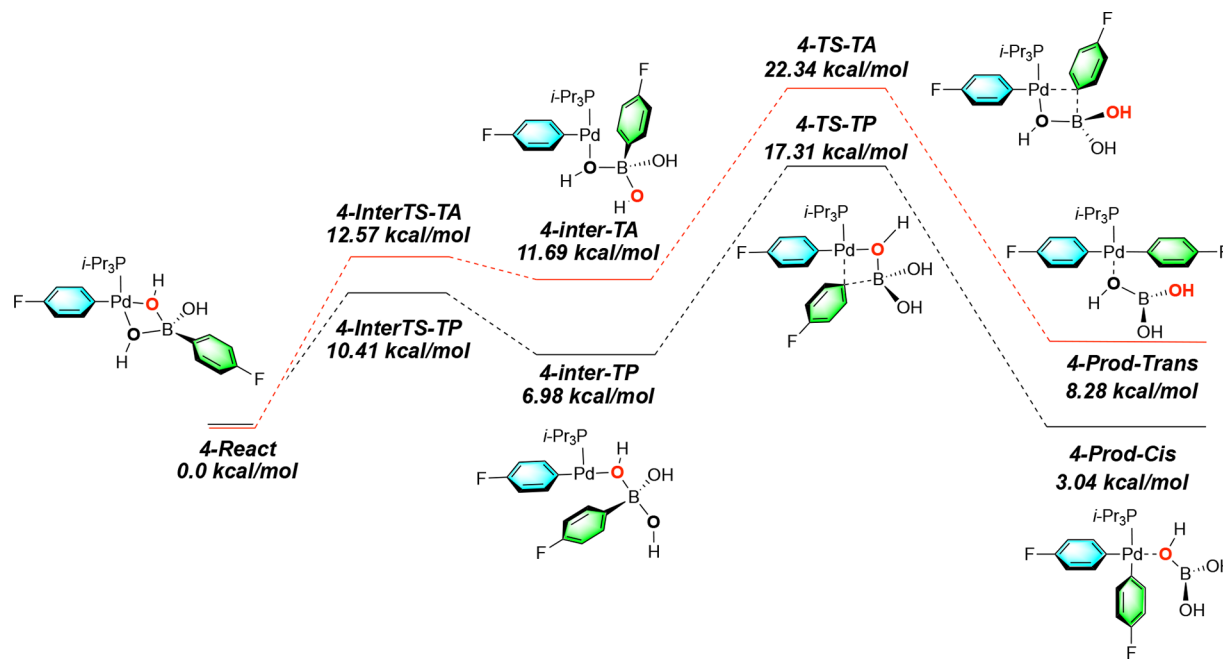


Figure 6. Calculated free energies for the reaction profile of boronic acid complex 4.

2.0 mol % of XPHOS-Pd-G3 and 1.0 equiv of 4-methylbromobenzene (**33**) formation of cross-coupling product **34** and the reappearance of glycol boronic ester **17** was observed in a ca. 1:1 ratio by ^{19}F NMR spectroscopy. We suspected that the reaction byproduct (2-hydroxy-1,3,2-dioxaborolane) was scavenging the hydroxide from **32** forming **35**. Therefore, increasing the amount of CsOH- H_2O from 1.0 to 3.0 led to the formation of cross-coupling product **34** in 96% yield (1.0 mmol scale) within 5 min at room temperature between **17**, **33**, and XPHOS-Pd-G3 (Scheme 7-2). This result clearly demonstrated that boronic esters can function directly as coupling partners under catalytic conditions.

4.4. Computational Analysis of the Reaction Profiles.

4.4.1. Previous Computational Studies on the Suzuki–Miyaura Reaction. Palladium catalyzed cross-coupling reactions have been extensively studied by a variety of computational methods.^{30,31} A forgoing computational study has evaluated monoligated structures similar to ours as intermediates in the Suzuki–Miyaura cross-coupling.³² In this study, the authors were able to predict the presence of the pretransmetalation intermediate we have experimentally observed, as well as predict the correct operative pathway. This study differed from our own in that the authors examine a triphenylphosphine ligated system, for which they predicted the rate-determining step to be Pd–O bond breakage in the monoligated species rather than transmetalation. The energy difference from the monolygated Pd–O–B linked structures and the transmetalation transition structure was calculated to be 7.4 kcal/mol, much lower than what has been calculated in this triisopropylphosphine ligated system.¹⁵ In order to achieve optimal results, we chose to survey of many functionals and employ a triple- ζ basis set to accurately reproduce the experimental thermochemical values. The LC- ω PBE functional was found to best replicate the experimental results.³³

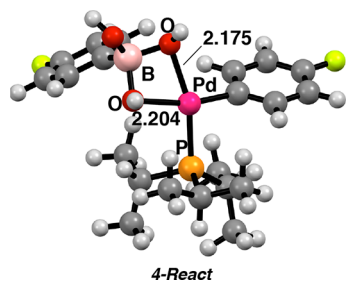
4.4.2. Computational Methods and Nomenclature. To gain further insight into the influence of the boronic ester moiety on the relative rates of transmetalation, the energy profiles for the boronic acid, the catechol ester, and the glycol ester (**4**, **8**, and

19) were examined computationally. The structures were optimized at the B3LYP-D3(BJ)/6-31G(d,p)/LANL2DZ level of theory, with energy calculations performed at the LC- ω PBE/Def2-TZVP level of theory with the CPCM solvation model (see the Supporting Information for complete description of computational details). Further, a more rigorous treatment of conformational analysis combined with a higher level of theory, compared to our previous publication,^{15b} yielded computationally derived activation parameters in very close agreement with the experimental data.³⁴

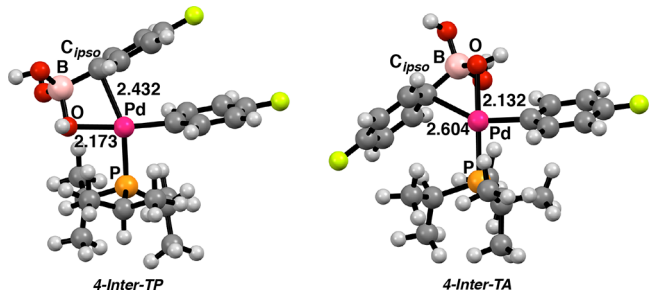
The energy profiles for the boronic acid, the catechol boronic ester, and the glycol boronic ester share common features and therefore a common nomenclature system has been devised. The monomeric palladium complexes with two Pd–O–B linkages are designated as reactants (*React*). The two different pathways by which Pd–O–B linkage is broken are uniquely defined, such that the pathway in which the scissile Pd–O bond is *trans* to the phosphine ligand is called “*TP*” and the pathway in which the scissile Pd–O bond is *trans* to the aryl ligand is called “*TA*”. The transition structures (*InterTS*) corresponding to the Pd–O bond breaking event are designated *InterTS-T(P/A)*. These transition structures lead to the pretransmetalation intermediates, which are designated as *inter-T(P/A)*. From here, the transmetalation transition structures (*TS*) are designated as *TS-T(P/A)*, and the products are named *Prod-cis* or *Prod-trans*, wherein *cis* and *trans* refers to the relative positions of the aryl ligands in the palladium coordination sphere.

4.4.3. Boronic Acid Energy Profile. Qualitatively, the computational results for the reaction profile for **4-React** agree with our previously published data (Figure 6). Because of the *trans* influence at palladium,³⁵ the oxygen ligands *trans* to the phosphine ligand and *trans* to the aryl ligand are nonequivalent. The Pd–O bond distance *trans* to the more strongly σ -donating aryl ligand is 2.204 Å, whereas the Pd–O bond distance *trans* to the more weakly donating phosphine ligand is 2.175 Å (Figure 7).

The transition state in which the Pd–O bond *trans* to the phosphine ligand (**4-InterTS-TP**) breaks is 2.16 kcal/mol lower

Figure 7. Nonequivalent Pd–O bond lengths in **4-React**.

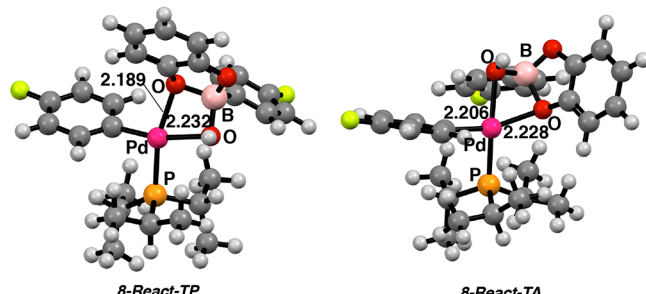
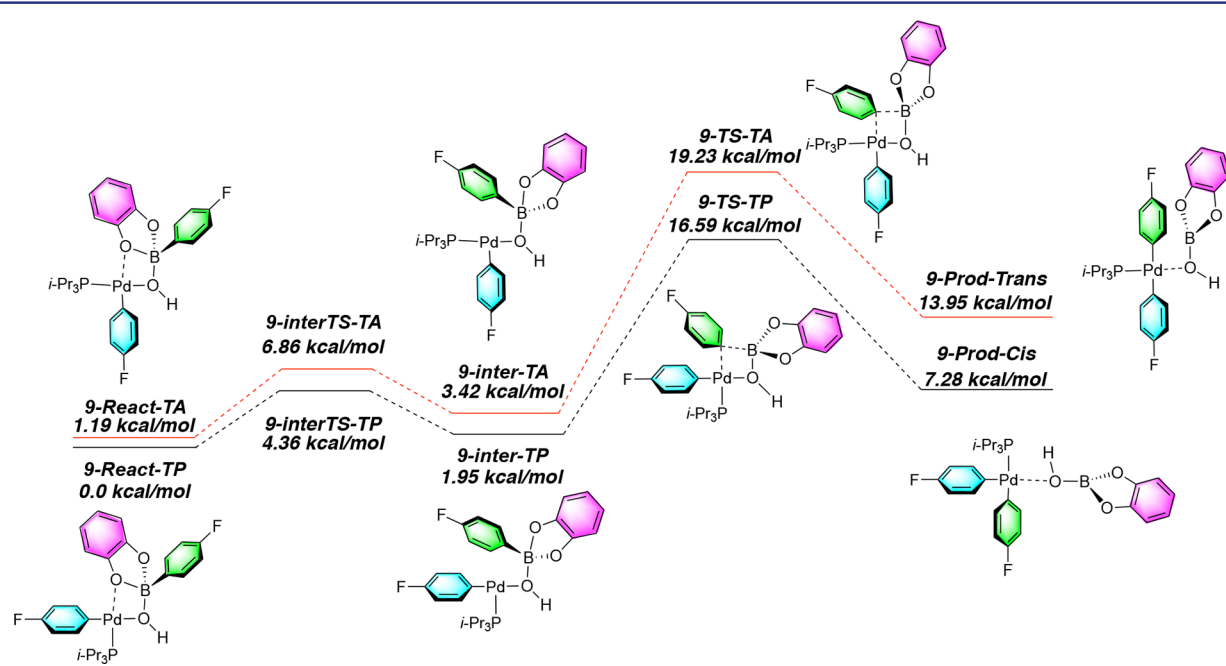
in energy than **4-InterTS-TA**, in which the Pd–O bond *trans* to the aryl ligand breaks. The movement associated with this transition barrier is a concerted Pd–O cleavage with precoordination of the migrating aryl group toward the palladium atom in a dihedral movement. As the TA pathway proceeds down this reaction coordinate, an unfavorable interaction develops between the arene of the boronic acid and the phosphine ligand. The TP pathway has no such interaction, resulting in a lower energy barrier. This destabilizing interaction is also present in the pretransmetalation intermediates (Figure 8): the more stable **4-inter-TP** structure (6.98 kcal/mol) has a

Figure 8. Attenuated Pd–O_{ipso} interaction in **4-inter-TA** (right) compared with **4-inter-TP** (left).

shorter Pd–C_{ipso} distance of 2.432 Å (where C_{ipso} is the *ipso* carbon of the boronate) than the **4-inter-TA** structure (11.69 kcal/mol, 2.604 Å), reflecting the disruption of this favorable interaction in the latter.

In agreement with our previously published results, the location of transition structures for transmetalation indicates that the *TP* pathway is operative. The calculated barrier height $\Delta G^\ddagger = 17.33$ kcal/mol is in close agreement with the experimentally measured barrier $\Delta G^\ddagger = 17.7$ kcal/mol at 243 K. In addition, rigorous conformational analysis of the triisopropylphosphine ligand revealed that the *TA* pathway is lower in energy than previously calculated (22.34 kcal/mol vs 25.06 kcal/mol). This accuracy suggests that the energies that cannot be measured experimentally (e.g., *InterTS* barriers, energies of intermediates) are also more reliable in these new calculations. Finally, calculations of steps after transmetalation were not performed, as they are after the rate-determining step and therefore are not kinetically relevant.

4.4. Catechol Ester Energy Profile. The energy profile for the catechol ester (Figure 9) begins with two possible reactants: one in which the hydroxyl group is *trans* to the aryl ligand (**9-React-TP**), and one in which the hydroxyl group is *trans* to the phosphine ligand (**9-React-TA**) (Figure 10). **9-React-TP** was

Figure 10. **9-React-TP** (left) and **9-React-TA** (right).Figure 9. Calculated free energies for the reaction profile of catechol ester complex **9**.

calculated to be 1.19 kcal/mol lower in energy than **9-React-TA**. As the hydroxyl ligand is likely a better σ -donor than the ester-oxygen owing to delocalization into the aromatic ring in the latter, the complex with the ester-oxygen *trans* to the aryl ligand is expected to be more thermodynamically stable due to the *trans* influence. This is contrary to what is observed computationally, and it is likely that **9-React-TA** is higher in energy because of an unfavorable steric interaction between the catechol ring the phosphine ligand despite the electronically more favorable ligand arrangement. However, the *trans* influence is still observable in the interatomic distances of the two Pd–O bonds. In **9-React-TP**, the Pd–O distance for the ester-oxygen *trans* to the phosphine ligand is 2.19 Å, whereas the hydroxyl-oxygen distance is 2.23 Å. Similarly, in **9-React-TA**, the hydroxyl-oxygen *trans* to the phosphine ligand has is 2.21 Å from the palladium atom, whereas the ester-oxygen is 2.28 Å from the palladium atom.

As in the boronic acid pathway, the **9-InterTS-TA** barrier (6.86 kcal/mol) is 2.5 kcal/mol higher in energy than the **9-InterTS-TP** barrier (4.36 kcal/mol), again resulting from the incipient unfavorable steric interaction in the **9-InterTS-TA** transition state which is absent in the **9-InterTS-TP** transition state. However, both barriers are much lower in energy than their analogs in the boronic acid energy profile, likely arising from the relatively weaker Pd–O interaction of the catechol ester oxygen again owing to the delocalization of the lone pairs into the adjacent aromatic ring. The **9-inter-TP** structure is 1.47 kcal/mol more stable than **9-inter-TA**, again resulting from the unfavorable interaction between the boronate aryl group and the phosphine in the latter, but is only 1.95 kcal/mol less stable the **9-React-TP**. The unfavorable steric interaction in **9-inter-TA** causes a longer Pd–C_{ipso} interatomic distance in **9-inter-TA** than in **9-inter-TP** (2.660 and 2.501 Å, respectively, Figure 11).

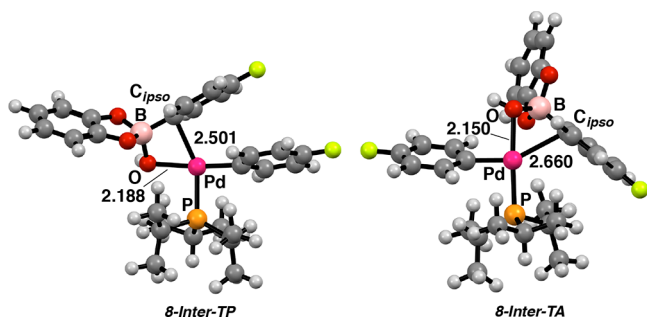


Figure 11. **9-Inter-TP** (left) and **9-Inter-TA** (right).

In the catechol boronic ester profile as well, the *TP* pathway ($\Delta G^\ddagger = 16.59$ kcal/mol calculated, $\Delta G^\ddagger = 17.04$ kcal/mol measured at 243 K) is operative, as the barrier to transmetalation for **9-TS-TP** is 2.94 kcal/mol lower in energy than that for the **8-TS-TA** pathway ($\Delta G^\ddagger = 19.23$ kcal/mol).

4.4.5. Glycol Ester Energy Profile. The energy profile for the glycol boronic ester also begins with two possible reactants, once again with the hydroxyl group either *trans* to the aryl ligand or the phosphine ligand. As expected, the *trans* influence in both **19-React-TP** and **19-React-TA** is observable (Figure 12). In **19-React-TP**, the Pd–O interatomic distance for the ester-oxygen *trans* to the more weakly donating phosphine ligand is 2.177 Å, whereas the hydroxyl-oxygen–palladium distance is 2.205 Å (Figure 13). These metrics follow the same trend in **19-React-TA**, such that the OH–Pd distance *trans* to the phosphine ligand 2.176 Å and the RO–Pd distance is 2.214 Å. In this case, the bond distances

indicate that the ester-oxygen is a more weakly binding ligand for palladium. This observation suggests that the energy differential between **19-React-TA** and **19-React-TP** of 0.97 kcal/mol is likely ascribable to the steric interaction between the glycol ester moiety and the triisopropylphosphine in **19-React-TA**.

The patterns for the relative energies of **19-InterTS-TA** and, **19-InterTS-TP** are similar to the previous cases, and the same rationales hold. Thus, **19-inter-TP** exhibits a closer Pd–C_{ipso} interaction (2.475 Å), whereas this interaction in **19-inter-TA** is attenuated by the steric interactions with the phosphine ligand (Pd–C_{ipso} interaction of 2.638 Å, Figure 14).

Here again, the **19-TS-TP** pathway is operative; the transition structure for transmetalation, $\Delta G^\ddagger = 16.02$ kcal/mol, is very close to the experimentally observed value of $\Delta G^\ddagger = 16.20$ kcal/mol at 243 K. The **19-TS-TA** transition state is calculated to be higher at $\Delta G^\ddagger = 18.96$ kcal/mol.

4.4.6. Comparison of Energy Profiles. The values for the experimentally measured activation energies have been reproduced computationally with striking accuracy. Thus, it is possible to speculate about the physical properties responsible for the rate differences of transmetalation for different boronates. According to our current hypothesis, three factors are responsible for the overall rate of reaction: (1) the ease of rehybridization of the boron atom, (2) the ease of formation of a coordinatively unsaturated palladium complex, and (3) migratory aptitude of the aryl group. Because all three precursors **2**, **8**, and **17** formed their respective 8-B-4 complexes **4**, **9**, and **19** quantitatively, the contribution from factor (1), to a first approximation can be considered negligible.³⁶ Factors (2) and (3) are primarily governed by the Lewis basicity of the boronate oxygen atoms which contribute to the energy of the reactant structure through modulation of the Pd–O interaction, and the delocalization of electron density to the *ipso* carbon of the migrating aryl group. All other factors being equal among the three systems (i.e., steric contributions, solvation) the interplay between these two factors is responsible for the relative rates of transmetalation. The discussion in this section is limited to only the *TP* structures, as they are on the operative pathway in all energy profiles.

To facilitate the comparison of the three profiles, they have been combined in a single chart approximately to scale (Figure 15). This view allows a clear analysis of the energetic requirements of the transmetalation elementary step. However, because the two key factors under consideration are the migratory aptitude of the aryl moiety and the stability of the intermediate, a more informative presentation of these comparisons involves normalization of the energies to the intermediate, *Inter-TP* (Figure 16). By normalizing the energy profiles to *Inter-TP*, the divergent contributions of the boronate ester oxygen atoms on the reactant energy and the migratory aptitude of the aryl ring are more clearly presented and can facilitate a better understanding of these contributions to the overall rate of the reaction.³⁷

The characteristics that point to the energy of the reactant structure as a deciding factor are (1) the interatomic distances of the Pd–O interactions (wherein O is the oxygen atom involved in the *InterTS-TP* bond-breaking event), (2) the energies of the transition structures that break those interactions, i.e., *InterTS-TP*, and (3) the energies of the *React-TP* and *Inter-TP* structures.

First, as bond distance often reflects bond strength, the relative Pd–O bond lengths can be used as a metric of the strength of the Pd–O interaction. In the series of profiles examined, the boronic acid and the glycol ester have the shortest Pd–O distances (2.175 and 2.177 Å, respectively), followed by the catechol ester (2.189

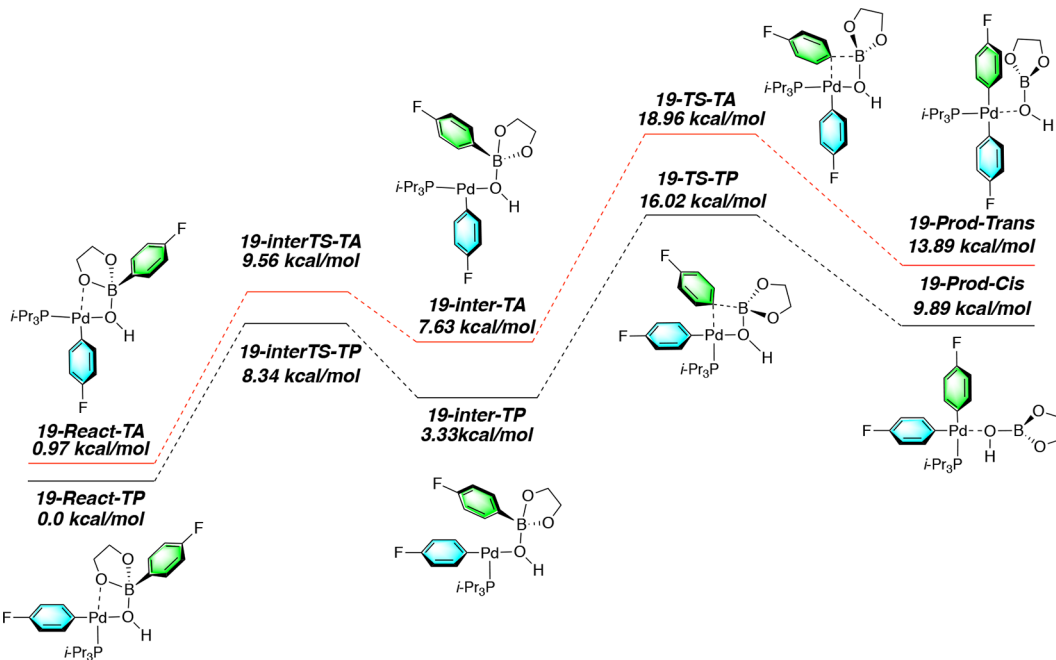


Figure 12. Calculated free energies for the reaction profile of glycol ester complex 19.

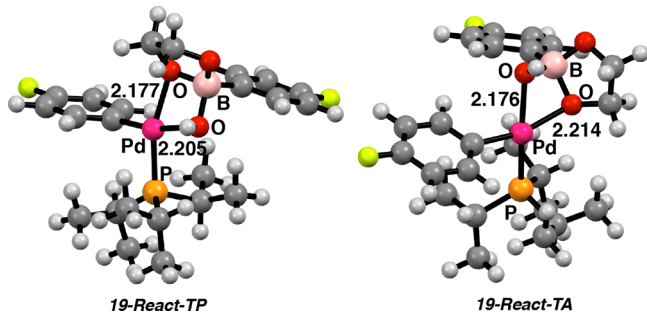


Figure 13. 19-React-TP (left) and 19-React-TA (right).

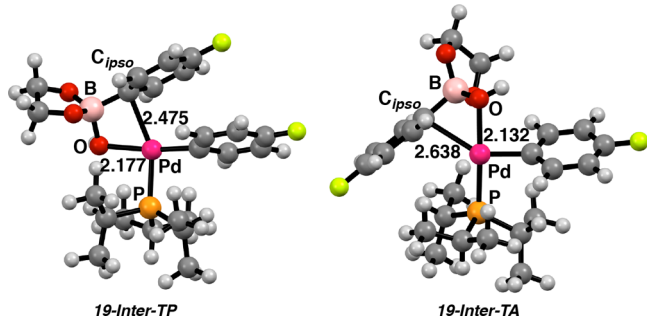


Figure 14. 19-inter-TP (left) and 19-inter-TA (right).

Å). Assuming that bond length and bond energy are closely related, it is likely that this trend also mirrors the stabilization of the complex according to the donicity of the bound oxygen, i.e., acid ~ glycol > catechol as shown in Figure 16. Second, the relative energy barriers of the Pd–O breaking events are also a metric of the strength of this interaction. The relative energies of the *InterTS-TP* barriers are boronic acid (10.41 kcal/mol) > glycol ester (8.34 kcal/mol) > catechol ester (4.36 kcal/mol). This trend is consistent with the previous analysis, in that the weakest Pd–O interaction (catechol ester) is the most easily dissociated, followed by the glycol ester, and then the boronic

acid. Third, the energies of the pretransmetalation intermediates (*inter-TP* and *inter-TA* structures) directly reflect the stability of these species. The intermediate structures all contain four bonding interactions to palladium: (1) the C–Pd σ -bond to the aryl residue, (2) the P–Pd bond to the phosphine ligand, (3) the O–Pd bond to the boronate, and (4) the C_{*ipso*}–Pd interaction to the migrating arene. These intermediate structures are energetically more similar to one another than the corresponding reactant structures, therefore the energy differentials between the intermediates and the reactants reflect reactant destabilization (Figure 15). For example, the 4-React-TP structure is 6.98 kcal/mol lower in energy than 4-*Inter-TP*, whereas the 9-React-TP structure is only 1.95 kcal/mol lower in energy than 9-*Inter-TP* (Figure 16). Therefore, the energetic penalty to form the pretransmetalation complex for the boronic acid is 5.03 kcal/mol greater than the energetic penalty encountered by the catechol ester. As a result, the overall barrier for transmetalation for the boronic acid is greater than for the catechol ester (Figure 15). Interestingly, analysis of the glycol ester and catechol ester energy profiles leads to a different conclusion. The glycol ester experiences an energetic penalty of 3.33 kcal/mol to form the pretransmetalation complex, 1.38 kcal/mol more than that encountered by the catechol ester (Figure 16). However, that difference is not consistent with the relative rates of transmetalation of the two esters. Therefore, a second factor influencing the elementary step of transmetalation must be considered to achieve a complete understanding of the individual contributions to the overall energy barrier.

The elementary step of transmetalation was defined above as the energy differential between the pretransmetalation complexes (*inter-TP*) and the respective *TS-TP* structures. The catechol ester displays the largest barrier for this elementary step (14.64 kcal/mol), followed by the glycol ester (12.69 kcal/mol), and finally the boronic acid (10.33 kcal/mol, Figure 16). However, as noted previously, the boronic acid has highest overall barrier (and experimentally is the slowest of the three, Figure 15) despite having the lowest energetic attribution for this elementary step. The magnitude of the energy barrier for this

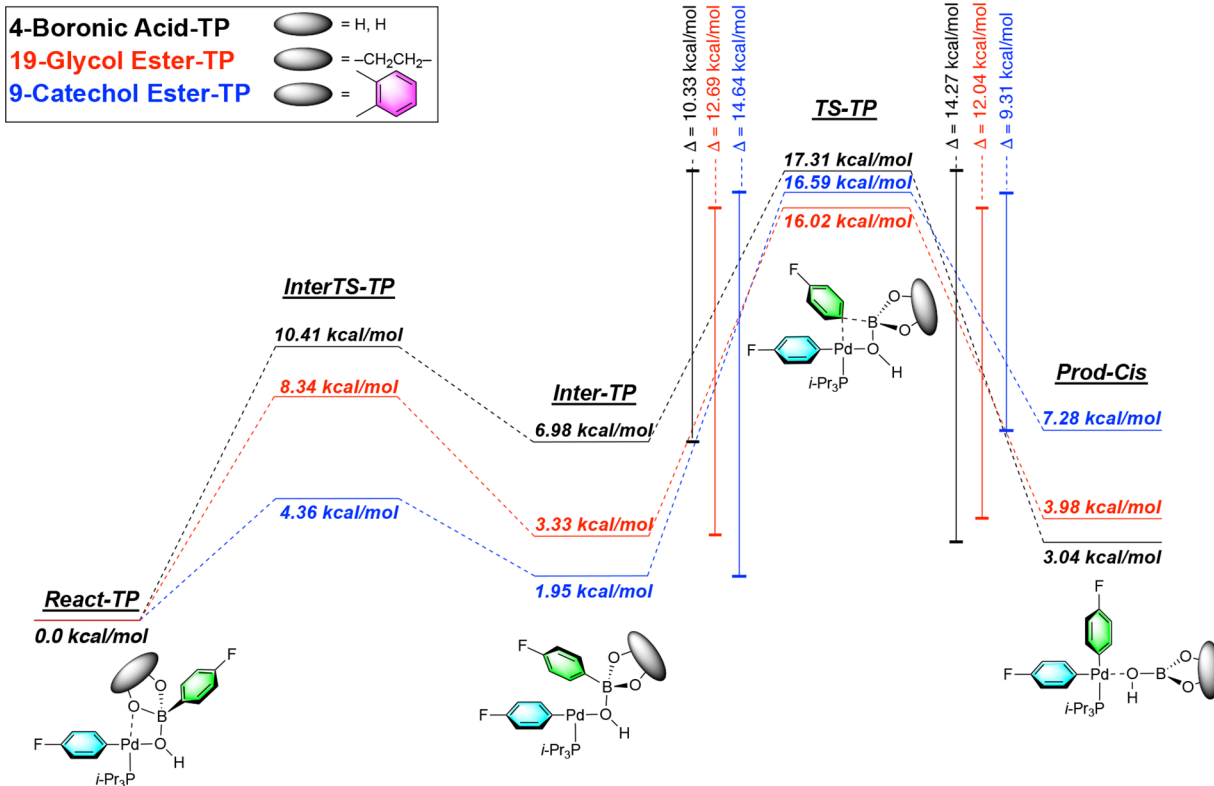


Figure 15. Comparison of the energy profiles for 4, 9, and 19.

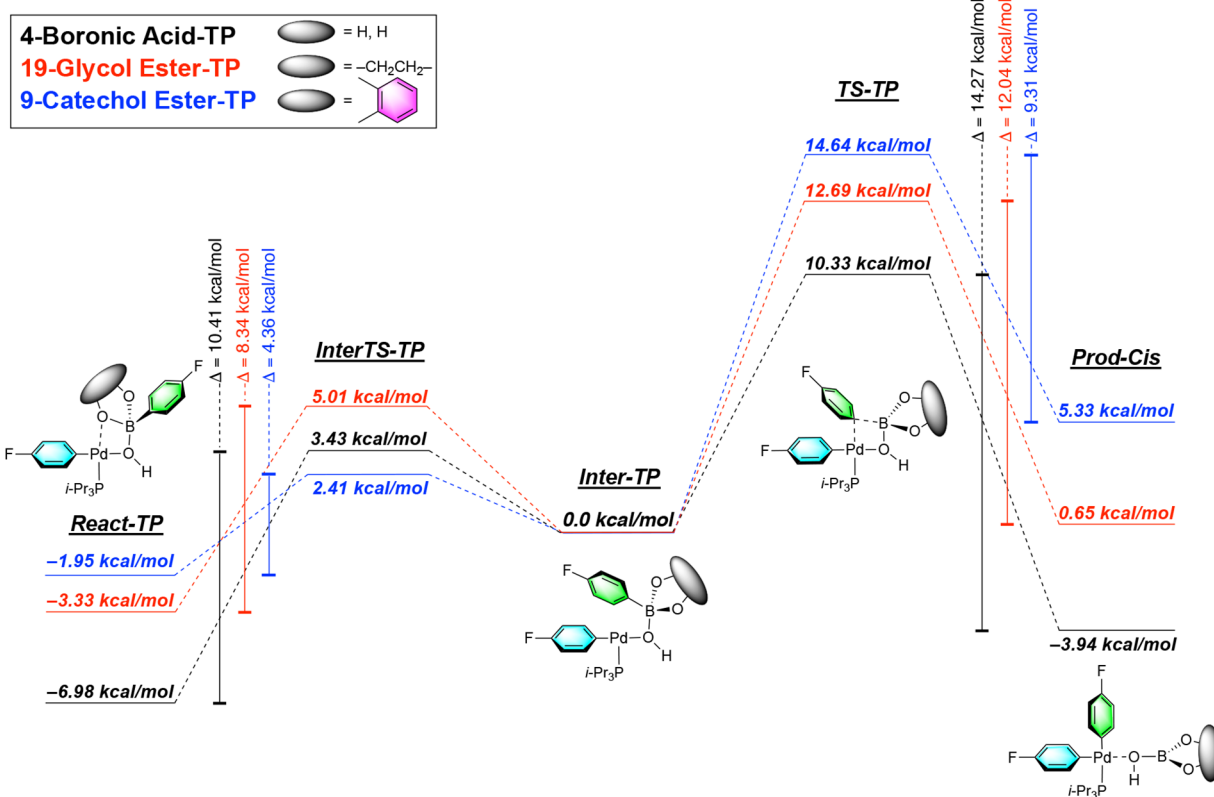


Figure 16. Comparison of the energy profiles for 4, 9, and 19 normalized to Inter-TP.

step is related to the migratory aptitude of the *ipso* carbon of the boronate moiety. In the case of the boronic acid, the hydroxyl units are free to rotate to provide optimal overlap with the $\sigma^*_{\text{B}-\text{C}}$

orbital (negative hyperconjugation),³⁸ thereby activating the arene for migration by increasing the electron density on this carbon.³⁹ This hyperconjugative activation is diminished slightly

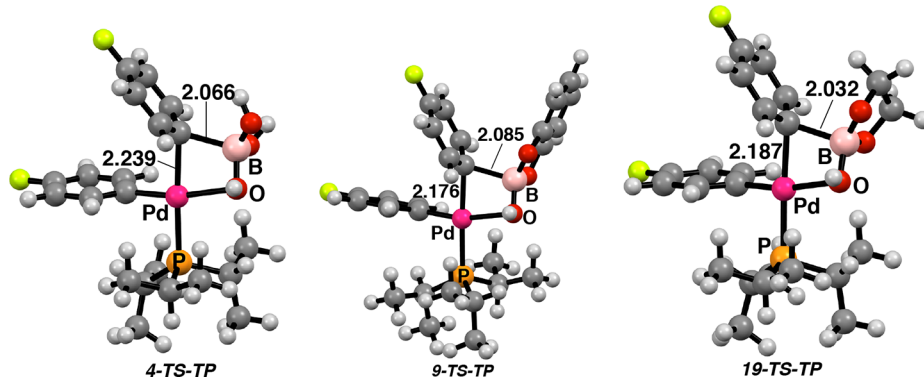


Figure 17. Transition state structures **4-TS-TP**, **9-TS-TP**, and **19-TS-TP**.

in the case of the glycol ester, as the geometric constraint induced by the five-membered ring distorts the overlap angle. Moreover, the five member ring enforces an anomeric effect in which the oxygen atoms of the glycol enjoy overlap with the opposing σ^*_{B-O} orbital, leading to less activation of the migratory arene with compared to the boronic acid. As a result, the elementary step for transmetalation in the glycol ester is less facile than for the boronic acid. Another possible contribution to this energy barrier is the torsional strain in the **19-TS-TP** structure between the hydrogens of the glycol ester resulting from the planarization of the five member ring (dihedral angles for the vicinal hydrogens are 27.28° and 26.71°). The catechol ester activates the migrating arene the least, as the electron density on the oxygens is delocalized through the adjacent aromatic system. This trend in migratory aptitude is reflected in the $B-C_{ipso}$ distance of the pretransmetalation intermediates; the boronic acid has the longest $B-C_{ipso}$ bond (1.656 \AA), the glycol ester has the second longest (1.635 \AA), and the catechol ester has the shortest (1.626 \AA) bond length. In this analysis, bond length can correlate with bond strength, which is inversely related to migratory aptitude (Figure 17).

By combining the above observations, it can be postulated that the relative overall energy barriers of transmetalation are a direct result of the interplay between reactant destabilization (E_{rd}) and the migratory aptitude of the transmetalating aryl group (E_{tm}). This gives the following simplified expression for the activation energy (E_{act}):

$$E_{act} = E_{rd} + E_{tm}$$

Because both of these factors are ultimately affected by the Lewis basicity of the boronate oxygens and they are inversely related. For example, more Lewis basic oxygens are capable of stabilizing the reactant through the $Pd-O$ interaction which leads to a higher activation barrier for dissociation and a less stable pretransmetalation intermediate thus disfavoring the generation of this intermediate. However, more Lewis basic oxygens can also increase the hyperconjugative activation of the migrating arene thus lowering the barrier to the elementary transmetalation event. The inverse relationship between E_{rd} and E_{tm} has curious consequences. By virtue of having more Lewis basic hydroxyl groups, the boronic acid minimizes E_{tm} , but the energy penalty encountered in the E_{rd} term results in the boronic acid having the highest E_{act} . The catechol ester has the lowest energy penalty E_{rd} but the resulting increase in E_{tm} offsets that advantage such that E_{act} is not a minimum. Finally, the glycol ester has the optimal balance of E_{rd} and E_{tm} of the esters examined, and therefore has the lowest overall activation energy.

5. CONCLUSIONS

For the first time, kinetically competent 8-B-4 complexes containing $Pd-O-B$ linkages “the missing links” between arylboronic esters and arylpalladium complexes in the Suzuki–Miyaura reaction have been observed and fully characterized by NMR spectroscopy. The characterization of these complexes was made possible by low temperature NMR spectroscopy with the NOE and HMBC experiments being crucial in solving the structures. Interestingly, various boronic esters such as catechol and glycol were found to undergo transmetalation with increased rates when compared to the arylboronic acid. Furthermore, a series of structural, kinetic, and computational investigations revealed two competing factors that are crucial for transmetalation to take place. First, the ability to access a coordinatively unsaturated palladium atom is crucial as demonstrated both kinetically and computationally for the catechol ester **8**. Second, the nucleophilic character of the $B-ipso$ carbon was also crucial for this event. Most importantly, glycol ester **17** was demonstrated to function under anhydrous catalytic conditions at room temperature, indicating that a prior hydrolysis step is not required for the transmetalation step. The influence of solvent, boron sources, and additives on catalytic reactions are currently under investigation and will be reported in due course.

■ ASSOCIATED CONTENT

S Supporting Information

The Supporting Information is available free of charge on the ACS Publications website at DOI: [10.1021/jacs.8b00400](https://doi.org/10.1021/jacs.8b00400).

Full experimental procedures and characterization data and copies of 1H , ^{13}C , ^{31}P , ^{19}F , ^{11}B , and NOESY spectra, along with full kinetic data ([PDF](#))

■ AUTHOR INFORMATION

Corresponding Author

*sdenmark@illinois.edu

ORCID

Andy A. Thomas: [0000-0001-6336-5566](https://orcid.org/0000-0001-6336-5566)

Scott E. Denmark: [0000-0002-1099-9765](https://orcid.org/0000-0002-1099-9765)

Notes

The authors declare no competing financial interest.

■ ACKNOWLEDGMENTS

We are grateful for generous financial support from the National Science Foundation (NSF-CHE1151566). A.A.T. is grateful to the University of Illinois and Eli Lilly for Graduate Fellowships.

We are grateful to the personnel in the support services (mass spectrometry, NMR spectroscopy, microanalysis) at the University of Illinois at Urbana–Champaign. Dr. Lingyang Zhu is especially thanked for helpful suggestions on NMR spectroscopy. Mr. Alexander Shved is thanked for preliminary experiments.

■ REFERENCES

- (1) (a) Roughley, S. D.; Jordan, A. M. *J. Med. Chem.* **2011**, *54*, 3451–3479. (b) Brown, D. G.; Boström, J. *J. Med. Chem.* **2016**, *59*, 4443–4458.
- (2) Hall, D. G. Structure, Properties, and Preparation of Boronic Acid Derivatives. *Boronic Acids*; Wiley-VCH Verlag GmbH & Co. KGaA: 2011; pp 1–133.
- (3) (a) Miyaura, N.; Yamada, K.; Suzuki, A. *Tetrahedron Lett.* **1979**, *20*, 3437–3440. (b) Miyaura, N.; Suzuki, A. *J. Chem. Soc., Chem. Commun.* **1979**, 866–867.
- (4) Miyaura, N.; Yanagi, T.; Suzuki, A. *Synth. Commun.* **1981**, *11*, 513–519.
- (5) Larsen, R. D.; King, A. O.; Chen, C. Y.; Corley, E. G.; Foster, B. S.; Roberts, F. E.; Yang, R. C.; Lieberman, D. R.; Reamer, R. A.; Tschaen, D. M.; Verhoeven, T. R.; Reider, P. J.; Lo, Y. S.; Rossano, L. T.; Brookes, A. S.; Meloni, D.; Moore, J. R.; Arnett, J. F.; et al. *J. Org. Chem.* **1994**, *59*, 6391–6394.
- (6) Dumrath, A.; Lübbe, C.; Beller, M. Palladium-Catalyzed Cross-Coupling Reactions – Industrial Applications. *Palladium-Catalyzed Coupling Reactions*; Wiley-VCH Verlag GmbH & Co. KGaA: 2013; pp 445–489.
- (7) Kruger, A. W.; Rozema, M. J.; Chu-Kung, A.; Gandarilla, J.; Haight, A. R.; Kotecki, B. J.; Richter, S. M.; Schwartz, A. M.; Wang, Z. *Org. Process Res. Dev.* **2009**, *13*, 1419–1425.
- (8) Stewart, G. W.; Brands, K. M. J.; Brewer, S. E.; Cowden, C. J.; Davies, A. J.; Edwards, J. S.; Gibson, A. W.; Hamilton, S. E.; Katz, J. D.; Keen, S. P.; Mullens, P. R.; Scott, J. P.; Wallace, D. J.; Wise, C. S. *Org. Process Res. Dev.* **2010**, *14*, 849–858.
- (9) De Koning, P. D.; McAndrew, D.; Moore, R.; Moses, I. B.; Boyles, D. C.; Kissick, K.; Stanchina, C. L.; Cuthbertson, T.; Kamatani, A.; Rahman, L.; Rodriguez, R.; Urbina, A.; Sandoval, A.; Rose, P. R. *Org. Process Res. Dev.* **2011**, *15*, 1018–1026.
- (10) (a) Cox, P. A.; Leach, A. G.; Campbell, A. D.; Lloyd-Jones, G. C. *J. Am. Chem. Soc.* **2016**, *138*, 9145–9157. (b) Molloy, J. J.; Clohessy, T. A.; Irving, C.; Anderson, N. A.; Lloyd-Jones, G. C.; Watson, J. B. *Chem. Sci.* **2017**, *8*, 1551–1559. (c) Cox, P. A.; Reid, M.; Leach, A. G.; Campbell, A. D.; King, E. J.; Lloyd-Jones, G. C. *J. Am. Chem. Soc.* **2017**, *139*, 13156–13165.
- (11) The masking term was defined by Lloyd Jones and co-workers: masking is distinct from “protection” because protection requires that a deprotection step take place prior to use. Lennox, A. J.; Lloyd-Jones, G. C. *Isr. J. Chem.* **2010**, *50*, 664–674.
- (12) (a) Lennox, A. J. J.; Lloyd-Jones, G. C. *J. Am. Chem. Soc.* **2012**, *134*, 7431–7441. (b) Lennox, A. J. J.; Lloyd-Jones, G. C. *Angew. Chem., Int. Ed.* **2012**, *51*, 9385–9388. (c) Butters, M.; Harvey, J. N.; Jover, J.; Lennox, A. J. J.; Lloyd-Jones, G. C.; Murray, M. *Angew. Chem., Int. Ed.* **2010**, *49*, 5156–5160. (c1) Lennox, A. J. J.; Lloyd-Jones, G. C. *Angew. Chem., Int. Ed.* **2013**, *52*, 7362–7370.
- (13) Gonzalez, J. A.; Ogba, O. M.; Morehouse, G. F.; Rosson, N.; Houk, K. N.; Leach, A. G.; Cheong, P. H. Y.; Burke, M. D.; Lloyd-Jones, G. C. *Nat. Chem.* **2016**, *8*, 1067–1075.
- (14) Lennox, A. J. J.; Lloyd-Jones, G. C. *Chem. Soc. Rev.* **2014**, *43*, 412–443.
- (15) (a) Thomas, A. A.; Denmark, S. E. *Science* **2016**, *352*, 329–332. (b) Thomas, A. A.; Wang, H.; Zahrt, A. F.; Denmark, S. E. *J. Am. Chem. Soc.* **2017**, *139*, 3805–3821. (c) Thomas, A. A.; Denmark, S. E. Ernest L. Eliel, a Physical Organic Chemist with the Right Tool for the Job: Rapid Injection Nuclear Magnetic Resonance. In *Stereochemistry and Global Connectivity: The Legacy of Ernest Eliel*; Cheng, H. N., Ed.; ACS Symposium Series; American Chemical Society: Washington, DC, 2018.
- (16) This classification designates N-X-L species where N is the number of formally valence-shell electrons about atom X, involved in bonding L ligands to X. Perkins, C. W.; Martin, J. C.; Arduengo, A. J.; Lau, W.; Alegria, A.; Kochi, J. K. *J. Am. Chem. Soc.* **1980**, *102*, 7753–7759.
- (17) See *Supporting Information* for all spectra and assignments of resonances.
- (18) Nöth, H.; Wrackmeyer, B. In *Nuclear Magnetic Resonance Spectroscopy of Boron Compounds*; Diehl, P., Fluck, E., Kosfeld, R., Eds.; NMR Basic Principles and Progress; Springer-Verlag, 1978; Vol. 14, Chapter 7, pp 74–100.
- (19) Furthermore, the ¹⁹F NMR signals remained as sharp singlets indicating that no dynamic process was evident. A similar result was observed for neopentyl 4-fluorophenylboronate ester **22**. Where a discrete intermediate was not observed; however, cross-coupling was observed.
- (20) This conclusion found support in the energies of the computationally derived structures wherein a 0.97 kcal/mol difference favoring **19** was calculated (see Section 4.4.5). The computationally predicted $K_{eq} = 0.134$ was very close to the experimentally observed equilibrium concentration $K_{eq} = 0.12$, ($K_{eq} = [19']/[19]$).
- (21) Furthermore, the ¹⁹F NMR chemical shifts for complex **6** in THF/CH₃OH were measured to be –121.01 ppm (F_a) and –118.33 ppm (F_b) suggesting a solvent effect for the measurement of these chemical shifts.
- (22) Because of peak broadening in certain 8-B-4 complexes and rapid formation of cross-coupling product **5** as a strong, sharp signal, the formation of **5** was found to be more reliable for determination of the rate.
- (23) The similarity of rates for appearance of **5** and consumption of **4** suggests that transmetalation is the rate-determining step for this process.
- (24) The sigmoidal curves made extraction of a comparable rate constant problematic and therefore were not fitted.
- (25) Driver, M. S.; Hartwig, J. F. *Organometallics* **1997**, *16*, 5706–7515.
- (26) The complexity of this system lends itself to other possible interpretations. We offer an explanation that is most consistent with all of the available data, but we cannot unambiguously exclude the possibility that the diminished rate of **21** relative to complex **4**, is the result of the inherent reactivity of complex **21**.
- (27) The inability to detect a discrete intermediate with boroxine **28** results from the multitude of boron-containing oligomers that precluded clear assignment of structure.
- (28) (a) Carrow, B. P.; Hartwig, J. F. *J. Am. Chem. Soc.* **2011**, *133*, 2116–2119. (b) Amatore, C.; Jutand, A.; Le Duc, G. *Chem. - Eur. J.* **2011**, *17*, 2492–2503. (c) Amatore, C.; Jutand, A.; Le Duc, G. *Angew. Chem.* **2012**, *124*, 1408–1411. (d) Schmidt, A. F.; Kurokhtina, A. A.; Larina, E. V. *Russ. J. Gen. Chem.* **2011**, *81*, 1573–1574.
- (29) We cannot unambiguously exclude the possibility that hydroxide forms a palladium hydroxide complex. These results do not contradict the conclusions of the studies described by Hartwig, and Amatore and Jutand (ref 28.)
- (30) Sperger, T.; Sanhueza, I.; Kalvet, I.; Schoenebeck, F. *Chem. Rev.* **2015**, *115*, 9532–9586 and references therein.
- (31) García-Melchor, M.; Braga, A. A. C.; Lledós, A.; Ujaque, G.; Maseras, F. *Acc. Chem. Res.* **2013**, *46*, 2626–2634.
- (32) Ortúñoz, M. A.; Lledós, A.; Maseras, F.; Ujaque, G. *ChemCatChem* **2014**, *6*, 3132–3138.
- (33) Calculations with the B3LYP-D3 and M06 functionals are given in the *Supporting Information* for comparison.
- (34) Besora, M.; Braga, A.; Ujaque, G.; Maseras, F.; Lledós, A. *Theor. Chem. Acc.* **2011**, *128*, 639–646.
- (35) Appleton, T. G.; Clark, H. C.; Manzer, L. E. *Coord. Chem. Rev.* **1973**, *10*, 335–422.
- (36) In ongoing studies, all of these contributing factors will be examined in a more thorough fashion by a comprehensive “energy decomposition analysis” of the intrinsic reaction coordinates of at least these three reactants. Hopffgarten, M. v.; Frenking, G. *WIREs Comput. Mol. Sci.* **2012**, *2*, 43–62.
- (37) Close inspection of the energies of the *Prod-TP* structures in Figure 16 shows that the diarylpalladium species **18-Prod-TP** is less

stable than its precursor, intermediate **18-Inter-TP** by 5.33 kcal/mol. A priori, this difference could suggest that the transmetalation is reversible and not the rate-limiting step. However, we are highly confident that the subsequent steps (dissociation of the boronic acid byproduct and reductive elimination) have much lower barriers than the reverse process, 9.31 kcal/mol. This feature will also be addressed in the in-depth computational analysis mentioned in ref 36.

- (38) Schleyer, P. v. R.; Kos, A. J. *Tetrahedron* **1983**, *39*, 1141–1150.
(39) Denmark, S. E.; Smith, R. C.; Chang, W.-t. T. *Tetrahedron* **2011**, *67*, 4391–4396.